Caramel UHF RFID Sensors for Pest Monitoring

Dmitry Dobrykh*, *Graduate Student Member*, Ilai Solomon, Hani Barhum, Denis Kolchanov, Or Messer, Maxim Sokol, Avigdor Drucker, Eran Socher, *Member, IEEE*, Alexey Slobozhanyuk, *Member, IEEE*, Dmitry Filonov, *Member, IEEE*, and Pavel Ginzburg, *Member, IEEE*

***Abstract* — The emerging need for green technologies motivates the development of new approaches to manufacture electronic consumables. In case of low-cost mass-production sensors, the problem becomes even more severe due to the generation of environmental waste. Here we demonstrate an RFID-type sensor based on a caramel substrate with a micron-scale conductive layer. The device, being primarily made of sugar, attracts insects, which consume it almost completely. As an application, we demonstrate a tag that can be applied for remote pest monitoring. In the experiment, a long-range UHF RFID communication channel is established and monitored over time. An RFID-on-caramel tag consumed by insects loses its connection with a reader, indicating the presence of pests. We show the new caramel-based devices to communicate with a reader over a 10-meter distance, paving the way to remote crop monitoring. Such low-cost biodegradable sensors are highly promising for smart agriculture, warehouse management, and stock monitoring approaches.**

***Index Terms* — RFID, sensors, pest monitoring, MXenes.**

I. INTRODUCTION

Green agricultural methods suggest reducing pesticide use to a minimum and considering local treatment only when required. For those endeavors, monitoring pests and rodents is highly desirable. Agricultural fields, greenhouses, and warehouses are among the places that can benefit from an autonomous inspection. For example, hundreds of billions of USDs, or around 20% of the world's food supply, are lost annually owing to pest and rodent activities [1]. Conventional chemical methods (pesticides) are not always suitable and profitable, which makes alternative monitoring and control measures an attractive alternative. Nowadays, pest control is carried out with a wide range of mechanical and biological techniques, including traps, or introducing natural enemies. New technological approaches are also introduced, including camera traps [2], [3], optical and acoustic sensors [4], [5], radar and lidar systems [6], [7], IoT-based systems [8], [9], and many others [10]–[15]. In most cases, the cost of those systems becomes an issue, setting additional tight constraints on the technology. Here, we will explore the capabilities of radio frequency identification (RFID) methods, where a tag can cost only a few cents.

RFID is a widely used technology for wireless identification of objects and contactless data readout, used in various practical applications, including logistics, retail, security, the Internet of Things, and many others [16]. This architecture is based on a passive low-cost tag and an active reader device that initiates the connection and processes data encoded on a modulated backscattered electromagnetic wave [17]. The design of a UHF (ultra-high frequency, ~920 MHz, depending on the licensing country) RFID tag is usually based on a metal dipole-like antenna on a thin flexible substrate to ensure fast convenient labeling. Although tags can be designed per application by tailoring the antenna properties. There are quite a few probable architectures, including patch antennas [18], PIFA antennas [19], slot antennas [20], and many others. Introducing new materials into RFID design enables new capabilities and significantly improves the existing performances. For example, MXenes, a family of two-dimensional (2D) transition metal carbides, carbonitrides and nitrides, are highly promising, as they allow manufacturing of lightweight RFID tags with micron-thin conductive layers [21]–[24]. Another example is high-index low-loss ceramic materials used for compact passive RFID tags with a long reading range [25], [26], omnidirectional response [27], [28], and improved hardware security [29]. Moreover, new dielectric materials could be used to integrate RFID technology and sensorics, e.g. [30], [31]. Smart RFID sensors are rapidly gaining attention in many different areas, including agriculture [32]. It is worth noting the increasing interest in the development of RFID devices with biodegradable materials to reduce the environmental footprint. Recently, bioresorbable substrates [33]–[35], biodegradable polymers [36], bioresorbable copper-based and zinc paints [37], [38], and edible and ingestible electronics[39]–[41] and other strategies

* ITMO team was supported by the Russian Science Foundation (Project 19-79-10232).

Dmitry Dobrykh, Hani Barhum, Denis Kolchanov, Pavel Ginzburg are with the School of Electrical Engineering, Tel Aviv University, Tel Aviv 69978, Israel. (email: dmitryd@mail.tau.ac.il, hanibarhum@mail.tau.ac.il, pginzburg@post.tau.ac.il)

Hani Barhum is with the Light-Matter Interaction Centre, Tel Aviv University, Tel Aviv, 69978, Israel

Hani Barhum is with the Triangle Regional Research and Development Center, Kfar Qara' 3007500, Israel

Ilai Solomon is with the Future Scientists Center–Alpha Program at Tel Aviv Youth University, Tel Aviv 6997801, Israel. (email: ilaisolomon1@gmail.com)

Or Messer, Maxim Sokol are with the Department of Materials Science and Engineering, Tel Aviv University, P.O.B 39040, Ramat Aviv 6997801, Israel. (email: ormesser@mail.tau.ac.il, sokolmax@tauex.tau.ac.il)

Avigdor Drucker, Eran Socher are with the Department of Physical Electronics, Tel Aviv University, Tel Aviv 69978, Israel. (email: avigdor2@tauex.tau.ac.il, socher@tauex.tau.ac.il)

Alexey Slobozhanyuk is with the School of Physics and Engineering, ITMO University, Saint Petersburg 197101, Russia (email: a.slobozhanyuk@metalab.ifmo.ru).

Dmitry Filonov is with the Center for Photonics and 2D Materials, Moscow Institute of Physics and Technology, Dolgoprudny 141700, Russia. (email: filonov.ds@mipt.ru)

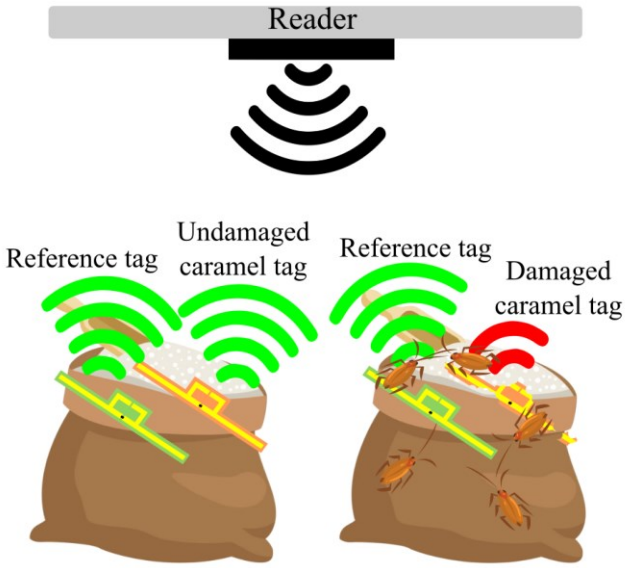

Fig. 1. Long-range interrogation of an edible RFID tag for pest monitoring. While an undamaged tag responds from a distance, a tag consumed by pests becomes unreadable. To enhance the detection reliability, an indestructible reference tag could be used to improve the reliability.

to bioenvironmental electronics have been considered.

Here we propose and demonstrate a concept of edible passive RFID tags for wireless monitoring of pests. Our architecture is based on a thin conductive antenna layer on a caramel substrate. The conductive layer is created by metal sputtering or with MXene for demonstrating several options. To maintain a wireless communication channel with a standard reader device, a commercial RFID integrated circuit (IC) (or chip) is used. The device operates as a UHF RFID long-range tag prior to interaction with pests. When pests, attracted by the sugar contains of the tag, consume the caramel substrate, thus destroying the conductive layer, they spoil the tag performance. After a critical point, the tag become unreadable. An uneatable tag can be introduced as a control tag to make the detection more reliable – Figure 1.

The manuscript is organized as follows: several tag designs and performance estimates are presented first, followed by manufacturing and testing. An outdoors experiment on the sensor operation is demonstrated before the Conclusion.

II. RFID-ON-CARAMEL DESIGN

A. RFID Tag Architecture

RFID tag consists of a small-footprint (~1 mm^2) integrated circuit (IC) and an antenna to support a wireless communication link. Regardless a vendor, ICs support the standardized communication channel. The antenna harvests electromagnetic energy sent by the reader and rectifies it partially to power the IC, which modulates the backscattered signal. The modulated reflection from the antenna holds the information about the tag. Typically, it is a static 96-bit number which, in a case of more advanced architectures, can be supplemented with additional information, e.g., local temperature, humidity and several others [32]. To provide these extra functionalities, a sensing element is required, elevating the cost and complexity of the design. Here we will concentrate on a static-number low-cost tag and adapt it to perform certain sensing operations. Our approach is to allow antenna characteristics to change upon interaction with pests. Then, the degradation of the antenna performance will impact the interrogation range, virtually making the long-range tag invisible. Another strategy can be a monitoring of the dropping in time (upon interaction with pests) received signal intensity, until the tag becomes unreadable.

Antenna elements are typically made of metals, capable to pick up free-space electromagnetic waves and transform them into conduction currents. However, metals are resistant to environmental changes and are not attractive for pests. Another important parameter governing the antenna performance is the substrate on which a metal structure is deposited. Substrates have dielectric responses, affecting the antenna impedance. Relying on the above, we will investigate RFID tag performances governed by (i) a damaged electromagnetic substrate and (ii) a damaged metal conductor. In practice, the damage will be associated with tag-pest interactions, promoted by introducing sugar into (i) the substrate material and/or (ii) conducting nanostructured bridges.

B. Dielectric Properties of Caramel

Prior to the electromagnetic design, we tested the dielectric properties of possible substrates. We explored caramel substrates fabricated by filling a mold with melted sugar. The electromagnetic properties (permittivity, ε) of these substrates were extracted with the hot-probe method, using an Agilent-85070E dielectric measurement kit. For precise system calibration and measurement control, in addition to the calibration kit (open, short, distilled water), a set of dielectric samples with known permittivity, including sugar powder, was used. The measurements were carried out for three caramel cylinders, each 6 cm in diameter and 2 cm in height. For every cylinder, we made five independent measurements in a narrow frequency band of 700-1200 MHz. At 900 MHz, the averaged permittivity was ~2.4 with the dielectric loss tangent ~0.04. We used this parameter for the design. Caramel properties were not retrieved in the past (at least we didn't find any reference for it), however, sugar was considered [42]. Sugar powder has lower density, and its permittivity is smaller.

C. Design and Optimization

We performed numerical modeling in CST Microwave Studio to estimate the performances of our RFID-on-caramel tags. We investigated three configurations with a standard widely employed dipole-like antenna architecture on different substrates, namely: (i) an FR-4 substrate, (ii) an FR-4 substrate partly replaced with caramel, and (iii) a full caramel substrate (see Fig. 1a). The layout of the antenna allows to obtain an impedance matching quite straightforwardly. The geometrical parameters of the designed tags were obtained with a parametric optimization (dipolar resonance and impedance matching) and are shown in Table 1. All three tags were dipole metallic (copper with losses) antennas with a T-shaped impedance matching element [43]. A 4.7 pF capacitor was plugged into each T-element to match the impedance to a commercial RFID

chip (Impinj Monza R6, datasheet impedance $Z = 14.1 - j148.6\ \Omega$). The metal strips were 19 μm thick. Instead of the additional lumped element in the T-match loop, the matching can be obtained by adjusting the length of the dipole and T-shaped element, which is more intentional and effective. Even though, keeping an additional degree of freedom might be used to compensate for probable fabrication imperfections.

TABLE I
GEOMETRICAL PARAMETERS OF THE RFID TAGS

Tag №	L1, mm	L2, mm	L3, mm	L4, mm	w, mm	Substrate thickness, mm
(i) Reference tag	115	20	7	-	3	1.6
(ii) Caramel bridge tag	115	20	7	20	3	1.6
(iii) Caramel substrate tag	120	20	7.5	-	3	1.5

To demonstrate the matching conditions, we performed the following numerical analysis. A numerical port with $Z = 14.1 - j148.6\ \Omega$ impedance was plugged in the gap of the tag antenna, and the complex reflection (S_{11} parameter) spectra were calculated. For the port impedance at the resonance, we used the value from the IC datasheet. Figure 2d demonstrates the numerically calculated $|S_{11}|$ spectra for three different realizations. Note that the antenna parameters ($L_{1,2,3,4}$) were optimized to provide matching within the RFID frequency band (here, 910 MHz was chosen).

After straightforward numerical optimization, all three realizations demonstrate excellent impedance matching with IC, nevertheless here is only a minor difference in geometrical parameters. Apart from the matching characteristics, there is a set of additional parameters that define the tag-reader communication channel.

To make a complete assessment, we calculated the realized gain, bandwidth, and estimated reading range for all three tags. The results are summarized in Table 2. The maximum reading range of the tags was calculated with the Friis model [44], [45]:

$$L_{max} = \frac{\lambda}{4\pi}\sqrt{\frac{P_t G_{TR} G_t}{P_{ch}}}, \quad (1)$$

where P_t is the power transmitted by the reader, G_{TR} is the gain of the reader Tx/Rx antenna, G_t is the realized gain of the tag's antenna, P_{ch} is the IC's sensitivity, and λ is the operating wavelength.

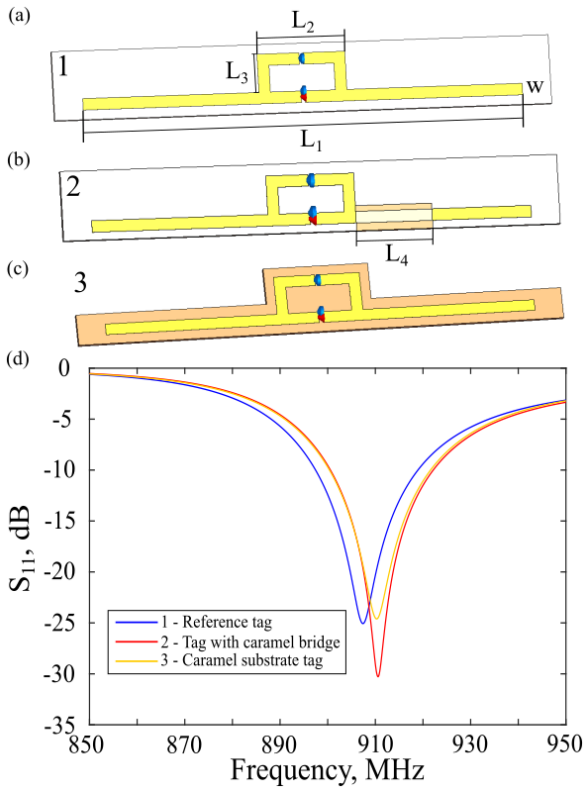

Fig. 2. Numerical assessment of the RFID tags' matching. Layouts of (a) tag on FR-4 dielectric substrate. (b) Tag on FR-4 substrate with a caramel bridge. (c) Tag on a caramel substrate. Systems' parameters are provided in Table 1. (d) The numerically calculated $|S_{11}|$ spectra of the RFID tags.

TABLE II
PARAMETERS OF THE RFID SYSTEM FOR LINK BUDGET CALCULATIONS

Tag №	P_t	G_{TR}	P_{ch}	G_t	L_{max}
(i) Reference tag	0.5 W (27 dBm)	5 (7 dBi)	-20 dBm	1.61 (2.10 dB)	15.9 m
(ii) Caramel bridge tag	0.5 W (27 dBm)	5 (7 dBi)	-20 dBm	1.62 (2.06 dB)	16 m
(iii) Caramel substrate tag	0.5 W (27 dBm)	5 (7 dBi)	-20 dBm	1.54 (1.88 dB)	15.6 m

D. Tag's Performance Degradation – Numerical Estimate

To estimate the impact of tags' reading range degradation resulting from insects chewing the caramel, we performed a set of numerical assessments. Figure 3a shows the calculated $|S_{11}|$ spectra for the 'caramel bridge' layout in two cases: tag is (i) undamaged and (ii) chewed-up. If the caramel substrate is removed, the conductive metal will collapse and dramatically affect the tag's performance, violating the impedance matching conditions in the relevant frequency range of 902-926 MHz. In this numerical example, to imitate the possible destruction, we removed from the structure a circular hole with a radius equal to the strip width. Figure 3b shows how impedance matching

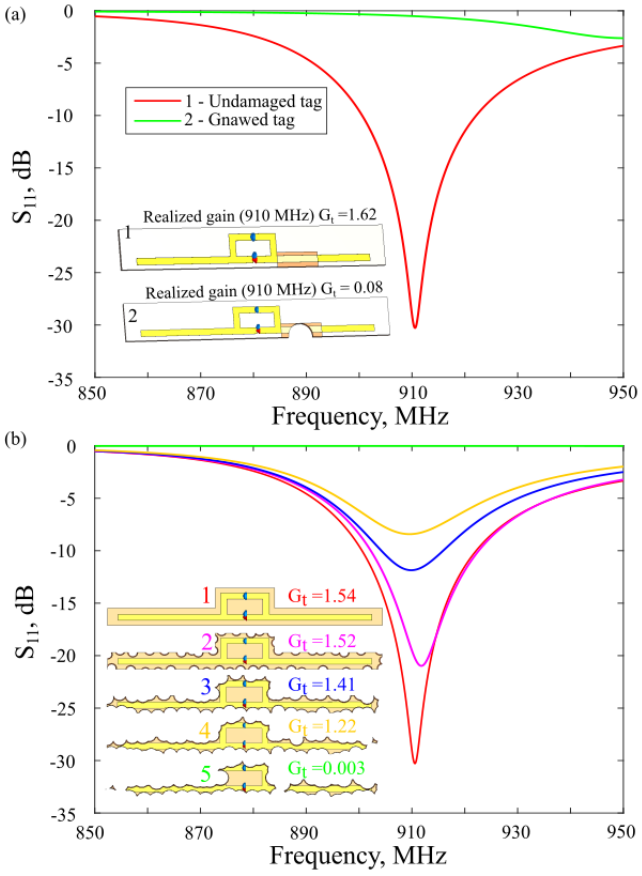

Fig. 3. $|S_{11}|$ spectra for: (a) tag with a caramel bridge: the chewed (green line) and undamaged ones (red line), (b) caramel substrate tag. Insets: scheme of the damaged and undamaged tags with correspoding realized gain at 910 MHz. Colored lines correspond to the different levels of tag destruction shown in the inset.

degrades as a caramel-substrate RFID tag is gradually destroyed (chewed). Here, we removed a set of circles with centers randomly distributed on the tag substrate. We investigated one realization of this type. While the conductive part of the antenna is intact, the tag's performance remains quite reasonable (see the realized gain parameter on insets 3-4 in Fig. 3b). The tag becomes mismatched only when the antenna is broken apart (inset 5). Antenna's realized gain appear in insets to Fig. 3, demonstrating the drop with the tag consumption.

The interrogation strategy can be several-fold, including a threshold approach or a continuous monitoring of the received signal strength. In the first case, the reader is placed at a range, which can be adjusted in a way that after certain damage the tag becomes unherdable. Advanced readers provide information on the received signal strength, which may be correlated with the tag's damage parameters after a set of statistical studies. In both cases, a standard non-consumable tag can be used as a reference, elevating the detection reliability. It is worth noting that pathloss in the communication channel depends on weather conditions and can be factored out given a reference.

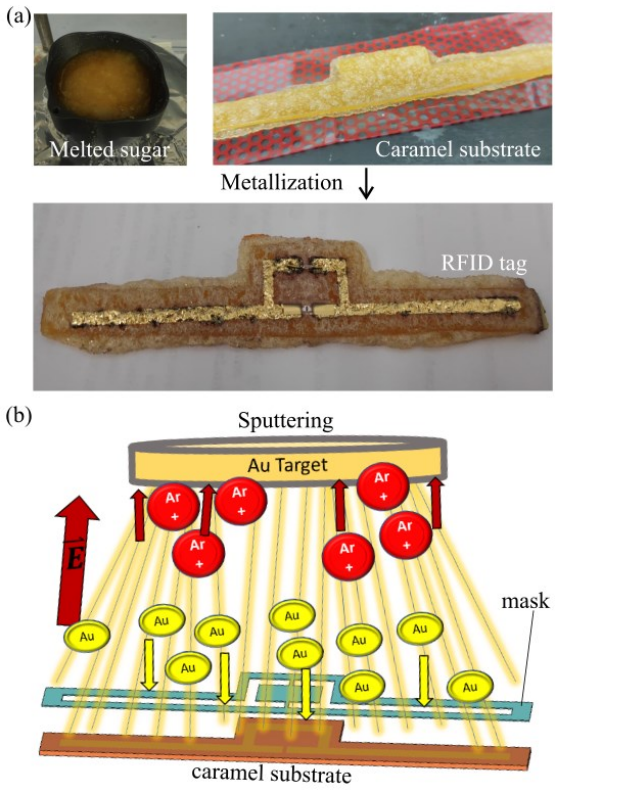

Fig. 4. (a) The fabrication process of RFID-on-caramel tag. (b) Schematic of a vacuum chamber metallization process: an inert gas plasma is accelerated on a gold target under high electric voltage, and a shadow mask is used to selectively deposit the metal.

III. TAGS FABRICATION

A. Tag on a Caramel Substrate

To fabricate substrates, we melted ordinary refined sugar on a heating plate and poured it into a mold, creating a 1.5 mm thick caramel layer (see Fig. 4a). The caramel substrate was dried in vacuum until a solid layer appeared. Crystallized sugar also appeared on the caramel surface when the water content was degassed. The next step is antenna deposition. While any low-cost metal can be used, we deposited a gold layer using the available equipment, a Penta magnetron. To create the desired metal shape, a shadow mask was made from a Kapton tape [46]. At this stage, the RFID IC and matching capacitor were soldered manually into the central gaps. Then, the substrate was placed into the sputtering vacuum chamber, and gold was deposited under 200 kV acceleration potential in inert gas plasma. We deposited a 1000 nm-thick Au film in three separate steps to prevent samples from overheating. Figure 4b shows a schematic illustration of the sputtering process.

B. Tag with a Caramel Bridge

While this fabrication method for a tag on a caramel substrate is well suited for proof-of-concept, it is rather complex and expensive for mass production. The numerical results prove that a small caramel bridge leads to almost the same performance of the tags. Furthermore, this layout will be more sensitive to pest appearance, as the caramel volume is reduced. Figure 5 shows

the fabrication process for an RFID tag with a caramel bridge.

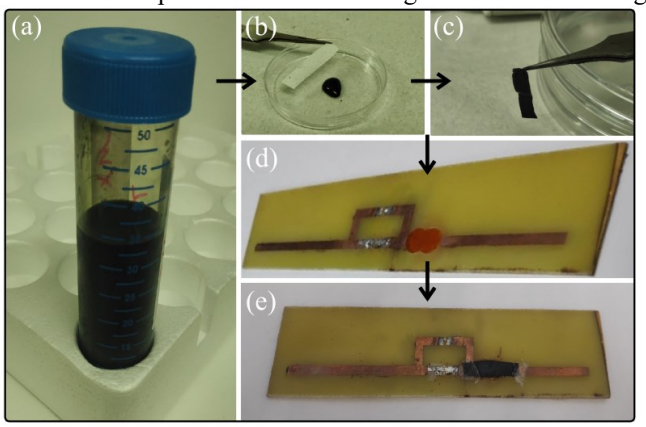

Fig. 5. Fabrication of a RFID tag with a caramel bridge. A MXene-based conductive strip is placed on a caramel spot. (a) MXene colloidal solution. (b-c) MXene impregnated thin paper. (d-e) RFID tag with a caramel spot before and after the addition of a conductive MXene layer.

A thin conductive strip placed on top of a caramel spot connects two parts of a standard printed antenna. In this case, when the caramel is consumed, the conductive bridge will be broken, leading to a significant drop of the received signal from the tag.

In principle, any conductive material can be used as a bridge on the caramel surface to supports RF current for antenna performance. The form factor of the caramel and the conductive part can be tuned per application, e.g., to match a certain pest population. Here we chose $Ti_3C_2T_z$ MXene as a conductor due to its very high conductivity (up to 10000 S/cm). In the last few years, this material platform has gained a great attention and demonstrated unique capabilities in many fields, including wireless communication devices [47]. MXene is considered safe, non-toxic and biocompatible, making it suitable for various applications [48]. The conductive strip was fabricated by leaving thin paper to soak in a colloidal solution of MXene at a concentration of 11 g/l (Fig. 5b). The MXene strip is 20 mm length, 3.5 mm width, and $\sim 50\ \mu m$ thickness. The next two paragraphs describe the synthesis process of the MXene [49].

C. *Synthesis of Ti_3AlC_2 MAX precursor*

The Ti_3AlC_2 powders were synthesized by mixing aluminium (Alfa Aesar, 99.5%, 325 mesh), titanium (Alfa Aesar, 99.5%, 325 mesh), and titanium carbide (Alfa Aesar, 99.5% 2 microns) powders in the following molar ratios: 1.15:1:2. The powders were mixed in a tumbler mixer at low rpm for 12 h before heating to 1450 °C for 3 h under flowing Ar. The partially sintered block was ground to a fine powder and filtered through a 400 mesh (38 µm) sieve, yielding particles with sizes ranging from 10 to 30 µm.

D. *Synthesis of $Ti_3C_2T_z$ MXene*

The Ti_3AlC_2 powder was etched in an HCl and LiF solution. First, 1 g of LiF (Alfa Aesar, 99.5%, 325 mesh) powder was dissolved in 10 mL of 12 M HCl (Fisher Scientific). Later, 1 g of the Ti_3AlC_2 powder was gradually added to the LiF-HCl solution and stirred for 24 h at 35°C. The obtained mixture was transferred into a 50 mL centrifuge vial for decantation of the acidic supernatant, and type I deionized (DI) water was added to fill the remaining volume. It was then centrifuged at 2300 RCF for 2 minutes, and the clear supernatant was removed. The washing procedure was repeated several times until the pH of the solution became higher than 6. At this point, DI water was added to the $Ti_3C_2T_z$ "clay," and the mixture was sonicated for 1 h under bubbling Ar. The bath temperature was kept at around 10°C, using ice to avoid oxidation. After centrifuging the solution for 1 h at 4700 RCF, the supernatant was pipetted off and sealed under Ar for storage before use. MXene with flake sizes in the range of 0.5-2 µm was obtained.

IV. EXPERIMENTAL DEMONSTRATION

After the design and manufacturing stages, we experimentally verified the concept. The experiment included three main steps: (i) measuring the maximum reading ranges for all the manufactured tags, (ii) leaving the tags to interact with insects outdoors, and (iii) re-measuring the reading range of all the tags. The tag's interrogation was performed with a commercial reader device model AS3992 LEO (a photograph of the experimental layout is shown in Fig. 6a). We also used a custom-made Yagi-Uda device (four directors) matched in the 890-930 MHz frequency range as a reader's antenna (see the inset in Fig. 6a). The antenna's gain is 7 dBi at 910 MHz. The transmitted power (P_t) was set to 27 dBm, which does not exceed 4 W of the Equivalent radiated power according to the international regulations for UHF RFID band.

To measure the maximal reading range tags were placed in the reader antenna's E-plane at a short cm-scale distance and carefully moved away until the received signal amplitude dropped below the reader's sensitivity. The reading count was updated every 5 seconds and the communication was considered successful if the tag was read at least 10 times within the specified time interval. It is worth noting that the maximal reading range depends on weather conditions and can drop with humidity increase, rain, etc. Consequently, assessing the caramel tag operation vs a reference and monitoring the received signal intensities at an intermediate reading is a preferable operation mode in future possible applications, which are better to consider warehouses scenarios with controllable environment. Furthermore, it is worth noting that sugar might accelerate pest activity. Thus, a potential use case can consider monitoring goods, which are themselves a subject to attraction, i.e., the tag does not provide a source for extra-lure.

As for any dipole-like RFID tag, the reading efficiency depends on the mutual polarization alignment between the reader the tag antennas. To compensate for the probable polarization mismatch in the azimuthal plane, a reader antenna with circular polarization might be used.

The tags were then distributed throughout the university campus, and interactions were recorded using a portable video camera. The experiment was carried out in Israel, where the warm climate encourages insect activity and allows for real-time observation of sugar-pest interactions. Ants, bugs, and cockroaches found the tags quite quickly and began to consume the caramel (see the second panel in Fig. 6c). After one hour, the sensitive MXene part of the tag was completely eaten away, while the tag on a caramel substrate was chewed up, and a

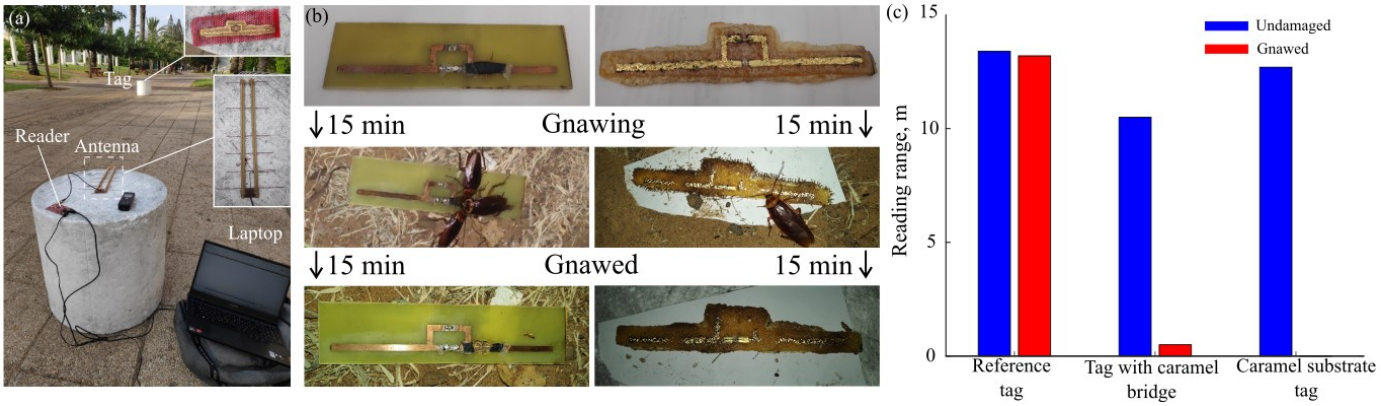

Fig. 6. (a) Photograph of the outdoors experimental setup: the RFID reader with a custom-made Yagi-Uda antenna interrogates tags from a distance. Insets show the tag and the antenna top view. (b) Diagrams of reading range of undamaged (blue) and gnawed (red) RFID tags. (c) A photograph of the tags evolution upon interaction with insects.

significant part of the metallization was destroyed. Worth noting that an accurate mapping of insects' activities requires implementing entomology-relevant protocols, e.g., [50].

After that, the maximum reading ranges of all the tags were re-measured. Figure 6b shows the bar diagrams of the maximal reading distance for all three tags before (blue) and after (red) they were chewed by insects. Following the obtained results, after the caramel bridge tag was chewed, its reading range decreased from 10.5 to 0.5 meters. The caramel substrate tag became unreadable due to the almost completely damaged antenna, while its initial reading range was 12.7 meters. The reading range of the reference tag obviously did not change within a small measurement error.

It is worth mentioning that the caramel tag lifetime strongly depends on the conditions. In indoor scenarios with low humidity and without interacting with insects, the tag is stable for months over the entire observation cycle. While the substrate properties might be affected by water absorption and oxidation, the antenna resonance is rather wide, mitigating the changes. Outdoors, given insects activity, it is naturally recycled within 1 day. Thus, apart from its clear sensorics advantages, the caramel tag concept becomes highly environmental. E.g., being used for labeling in a warehouse, it is naturally recycled outdoors with a day-scale timeline almost without leaving leftovers.

V. CONCLUSION

The concept of an edible RFID tag for pest monitoring has been developed and demonstrated in several configurations. The key approach is adding sugar-containing elements to the antenna design, making this wireless device prone to environmental-dependent degradation. In particular, caramel inclusions were introduced within an RFID antenna as substrate elements, making the tag a target for insects. We have demonstrated two main architectures, in which (i) the entire tag is located on a caramel substrate and (ii) two parts of the tag are connected by a caramel bridge with a conductor. Both configurations proved to be efficient for pest monitoring. While the first realization led to a complete violation of wireless communication with the tag, the second case exhibited a significant drop in the interrogation range. Several fabrication strategies have been presented, including metal sputtering and colloidal deposition of an MXene strip. The later approach also provides a future opportunity of developing a flexible and low-cost sensor platform, which is essential for assessing future RFID applications, which, however, require a set of additional performance checkups. The reliability of the detection method can be improved by introducing a reference (uneatable) tag, which serves as a reference bit. Apart from pest monitoring, creating electromagnetic devices on eco-friendly platforms contributes to the general endeavor to promote green technologies with biodegradable components. This concept is vital for cheap consumable devices that are mass produced and can lead to waste generation. In this case, recycling becomes a critical issue, and its costs might exceed the manufacturing costs.

AKNOWLEGEMENTS

The authors thank Lydia Pogorelskaya for her critical reading of the manuscript and useful suggestions.

REFERENCIES:

[1] A. W. E.C. Oerke, H.W. Dehne, F. Schönbeck, *Crop Production and Crop Protection: Estimated Losses in Major Food and Cash Crops*, Elsevier S. Amsterdam, 1994.

[2] D. Rassati, M. Faccoli, F. Chinellato, S. Hardwick, D. M. Suckling, and A. Battisti, "Web-based automatic traps for early detection of alien wood-boring beetles," *Entomol. Exp. Appl.*, vol. 160, no. 1, pp. 91–95, Jul. 2016, doi: 10.1111/EEA.12453.

[3] M. Preti, F. Verheggen, and S. Angeli, "Insect pest monitoring with camera-equipped traps: strengths and limitations," *J. Pest Sci. (2004).*, vol. 94, no. 2, pp. 203–217, Mar. 2021, doi: 10.1007/s10340-020-01309-4.

[4] S. Azfar *et al.*, "Monitoring, Detection and Control Techniques of Agriculture Pests and Diseases using Wireless Sensor Network: A Review," *Int. J. Adv. Comput. Sci. Appl.*, vol. 9, no. 12, pp. 424–433, 2018, doi: 10.14569/IJACSA.2018.091260.

[5] C. Kirkeby *et al.*, "Advances in automatic identification of flying

insects using optical sensors and machine learning," *Sci. Reports 2021 111*, vol. 11, no. 1, pp. 1–8, Jan. 2021, doi: 10.1038/s41598-021-81005-0.

[6] M. Dwivedi, M. H. Shadab, and V. R. Santosh, "Insect pest detection, migration and monitoring using radar and LiDAR systems," *Innov. Pest Manag. Approaches 21st Century Harnessing Autom. Unmanned Technol.*, pp. 61–76, Mar. 2020, doi: 10.1007/978-981-15-0794-6_4/COVER.

[7] A. Noskov, J. Bendix, and N. Friess, "A Review of Insect Monitoring Approaches with Special Reference to Radar Techniques," *Sensors 2021, Vol. 21, Page 1474*, vol. 21, no. 4, p. 1474, Feb. 2021, doi: 10.3390/S21041474.

[8] D. O. Kiobia, C. J. Mwitta, K. G. Fue, J. M. Schmidt, D. G. Riley, and G. C. Rains, "A Review of Successes and Impeding Challenges of IoT-Based Insect Pest Detection Systems for Estimating Agroecosystem Health and Productivity of Cotton," *Sensors 2023, Vol. 23, Page 4127*, vol. 23, no. 8, p. 4127, Apr. 2023, doi: 10.3390/S23084127.

[9] A. Vangala, A. K. Das, N. Kumar, and M. Alazab, "Smart Secure Sensing for IoT-Based Agriculture: Blockchain Perspective," *IEEE Sens. J.*, vol. 21, no. 16, pp. 17591–17607, Aug. 2021, doi: 10.1109/JSEN.2020.3012294.

[10] O. López, M. M. Rach, H. Migallon, M. P. Malumbres, A. Bonastre, and J. J. Serrano, "Monitoring Pest Insect Traps by Means of Low-Power Image Sensor Technologies," *Sensors 2012, Vol. 12, Pages 15801-15819*, vol. 12, no. 11, pp. 15801–15819, Nov. 2012, doi: 10.3390/S121115801.

[11] D. J. A. Rustia, C. E. Lin, J. Y. Chung, Y. J. Zhuang, J. C. Hsu, and T. Te Lin, "Application of an image and environmental sensor network for automated greenhouse insect pest monitoring," *J. Asia. Pac. Entomol.*, vol. 23, no. 1, pp. 17–28, Apr. 2020, doi: 10.1016/J.ASPEN.2019.11.006.

[12] M. E. Bayrakdar, "A Smart Insect Pest Detection Technique with Qualified Underground Wireless Sensor Nodes for Precision Agriculture," *IEEE Sens. J.*, vol. 19, no. 22, pp. 10892–10897, Nov. 2019, doi: 10.1109/JSEN.2019.2931816.

[13] S. Cui, P. Ling, H. Zhu, and H. M. Keener, "Plant Pest Detection Using an Artificial Nose System: A Review," *Sensors 2018, Vol. 18, Page 378*, vol. 18, no. 2, p. 378, Jan. 2018, doi: 10.3390/S18020378.

[14] D. Marković, D. Vujičić, S. Tanasković, B. Đorđević, S. Ranđić, and Z. Stamenković, "Prediction of Pest Insect Appearance Using Sensors and Machine Learning," *Sensors 2021, Vol. 21, Page 4846*, vol. 21, no. 14, p. 4846, Jul. 2021, doi: 10.3390/S21144846.

[15] H. Liu, S. H. Lee, and J. S. Chahl, "A Multispectral 3-D Vision System for Invertebrate Detection on Crops," *IEEE Sens. J.*, vol. 17, no. 22, pp. 7502–7515, Nov. 2017, doi: 10.1109/JSEN.2017.2757049.

[16] S. B. Miles, S. Sarma, and J. R. Williams, *RFID Technology and Applications*, vol. 9780521880. Cambridge: Cambridge University Press, 2008.

[17] D. Dobkin, *The RF in RFID: Passive UHF RFID in Practice*. Oxford: Elsevier, 2007.

[18] Z. Wang, S. Fang, S. Fu, and S. Jia, "Single-fed broadband circularly polarized stacked patch antenna with horizontally meandered strip for universal UHF RFID applications," *IEEE Trans. Microw. Theory Tech.*, vol. 59, no. 4 PART 2, pp. 1066–1073, Apr. 2011, doi: 10.1109/TMTT.2011.2114010.

[19] W. Choi, H. W. Son, J. H. Bae, G. Y. Choi, C. S. Pyo, and J. S. Chae, "An RFID tag using a planar inverted-f antenna capable of being stuck to metallic objects," *ETRI J.*, vol. 28, no. 2, pp. 216–218, 2006, doi: 10.4218/etrij.06.0205.0082.

[20] K. H. Lin, S. L. Chen, and R. Mittra, "A capacitively coupling multifeed slot antenna for metallic RFID tag design," *IEEE Antennas Wirel. Propag. Lett.*, vol. 9, pp. 447–450, 2010, doi: 10.1109/LAWP.2010.2048991.

[21] Y. Shao *et al.*, "Room-temperature high-precision printing of flexible wireless electronics based on MXene inks," *Nat. Commun. 2022 131*, vol. 13, no. 1, pp. 1–8, Jun. 2022, doi: 10.1038/s41467-022-30648-2.

[22] A. VahidMohammadi, J. Rosen, and Y. Gogotsi, "The world of two-dimensional carbides and nitrides (MXenes)," *Science*, vol. 372, no. 6547, Jun. 2021, doi: 10.1126/SCIENCE.ABF1581.

[23] M. Han *et al.*, "Solution-Processed Ti3C2Tx MXene Antennas for Radio-Frequency Communication," *Adv. Mater.*, vol. 33, no. 1, p. 2003225, Jan. 2021, doi: 10.1002/ADMA.202003225.

[24] K. Khorsand Kazemi *et al.*, "Low-Profile Planar Antenna Sensor Based on Ti3C2Tx MXene Membrane for VOC and Humidity Monitoring," *Adv. Mater. Interfaces*, vol. 9, no. 13, p. 2102411, May 2022, doi: 10.1002/ADMI.202102411.

[25] D. Dobrykh *et al.*, "Long-Range Miniaturized Ceramic RFID Tags," *IEEE Trans. Antennas Propag.*, vol. 69, no. 6, pp. 3125–3131, 2021, doi: 10.1109/TAP.2020.3037663.

[26] I. Yusupov, D. Dobrykh, D. Filonov, A. Slobozhanyuk, and P. Ginzburg, "Miniature Long-Range Ceramic On-Metal RFID Tag," *IEEE Trans. Antennas Propag.*, vol. 70, no. 11, pp. 10226–10232, Nov. 2022, doi: 10.1109/TAP.2022.3195551.

[27] A. Mikhailovskaya *et al.*, "Omnidirectional miniature RFID tag," *Appl. Phys. Lett.*, vol. 119, no. 3, p. 033503, Jul. 2021, doi: 10.1063/5.0054740.

[28] D. Dobrykh, I. Yusupov, P. Ginzburg, A. Slobozhanyuk, and D. Filonov, "Self-aligning roly-poly RFID tag," *Sci. Reports 2022 121*, vol. 12, no. 1, pp. 1–7, Feb. 2022, doi: 10.1038/s41598-022-06061-6.

[29] D. Dobrykh, D. Filonov, A. Slobozhanyuk, and P. Ginzburg, "Hardware RFID Security for Preventing Far-Field Attacks," *IEEE Trans. Antennas Propag.*, vol. 70, no. 3, pp. 2199–2204, Mar. 2022, doi: 10.1109/TAP.2021.3118846.

[30] I. Yusupov, D. Filonov, A. Bogdanov, P. Ginzburg, M. V. Rybin, and A. Slobozhanyuk, "Chipless wireless temperature sensor based on quasi-BIC resonance," *Appl. Phys. Lett.*, vol. 119, no. 19, p. 193504, Nov. 2021, doi: 10.1063/5.0064480.

[31] A. J. R. Hillier, V. Makarovaite, C. W. Gourlay, S. J. Holder, and J. C. Batchelor, "A Passive UHF RFID Dielectric Sensor for Aqueous Electrolytes," *IEEE Sens. J.*, vol. 19, no. 14, pp. 5389–5395, Jul. 2019, doi: 10.1109/JSEN.2019.2909353.

[32] F. Costa, S. Genovesi, M. Borgese, A. Michel, F. A. Dicandia, and G. Manara, "A review of rfid sensors, the new frontier of internet of things," *Sensors*, vol. 21, no. 9, 2021, doi: 10.3390/s21093138.

[33] D. Gupta, D. Sood, M. Yu, and M. Kumar, "Compact Biodegradable UHF RFID Tag for Short Life Cycle Applications," *2021 IEEE Indian Conf. Antennas Propagation, InCAP 2021*, pp. 399–401, 2021, doi: 10.1109/INCAP52216.2021.9726482.

[34] J. Morales-Guerra, F. Umana-Idarraga, W. Giraldo-Escobar, E. Gonzalez-Valencia, and E. Reyes-Vera, "Performance analysis of a Compact, Flexible and Biodegradable UHF RFID Tag Antenna," *2021 Int. Conf. Electromagn. Adv. Appl. ICEAA 2021*, pp. 357–360, Aug. 2021, doi: 10.1109/ICEAA52647.2021.9539617.

[35] M. Fantuzzi, D. Masotti, and A. Costanzo, "A Novel Integrated UWB-UHF One-Port Antenna for Localization and Energy Harvesting," *IEEE Trans. Antennas Propag.*, vol. 63, no. 9, pp. 3839–3848, Sep. 2015, doi: 10.1109/TAP.2015.2452969.

[36] A. Mehmood, X. Chen, H. He, S. Ma, L. Ukkonen, and J. Virkki, "Intelligent Wristbands - Fabrication of Wearable RFID Solutions by 3D Printing Pen," *2020 IEEE Int. Symp. Antennas Propag. North Am. Radio Sci. Meet. IEEECONF 2020 - Proc.*, pp. 1319–1320, Jul. 2020, doi: 10.1109/IEEECONF35879.2020.9329572.

[37] M. Kumar, A. Sharma, and I. J. G. Zuazola, "A biodegradable multi-platform tolerant passive UHF RFID tag antenna for short-life cycle IoT applications," *2021 IEEE Indian Conf. Antennas Propagation, InCAP 2021*, pp. 391–394, 2021, doi: 10.1109/INCAP52216.2021.9726371.

[38] Y. Sui *et al.*, "A Reactive Inkjet Printing Process for Fabricating Biodegradable Conductive Zinc Structures," *Adv. Eng. Mater.*, vol. 25, no. 1, p. 2200529, Jan. 2023, doi: 10.1002/ADEM.202200529.

[39] A. S. Sharova, F. Melloni, G. Lanzani, C. J. Bettinger, and M. Caironi, "Edible Electronics: The Vision and the Challenge," *Adv. Mater. Technol.*, vol. 6, no. 2, p. 2000757, Feb. 2021, doi: 10.1002/ADMT.202000757.

[40] Y. Wu *et al.*, "Edible and Nutritive Electronics: Materials, Fabrications, Components, and Applications," *Adv. Mater. Technol.*, vol. 5, no. 10, p. 2000100, Oct. 2020, doi: 10.1002/ADMT.202000100.

[41] S.-Y. Yang *et al.*, "Powering Implantable and Ingestible Electronics," *Adv. Funct. Mater.*, vol. 31, no. 44, p. 2009289, Oct. 2021, doi: 10.1002/ADFM.202009289.

[42] J. Peltonen, M. Murtomaa, K. Robinson, and J. Salonen, "The electrical resistivity and relative permittivity of binary powder mixtures," *Powder Technol.*, vol. 325, pp. 228–233, Feb. 2018, doi: 10.1016/J.POWTEC.2017.10.060.

[43] J. Xi and H. Zhu, "UHF RFID impedance matching: T-match-dipole tag design on the highway," *2015 IEEE Int. Conf. RFID, RFID 2015*, pp. 86–93, May 2015, doi: 10.1109/RFID.2015.7113077.

[44] S. S. Srikant and R. P. Mahapatra, "Read Range of UHF Passive RFID," *Int. J. Comput. Theory Eng.*, pp. 323–325, 2010, doi: 10.7763/ijcte.2010.v2.160.

[45] K. V. S. Rao, P. V. Nikitin, and S. F. Lam, "Antenna design for UHF RFID tags: a review and a practical application," *IEEE Trans. Antennas Propag.*, vol. 53, no. 12, pp. 3870–3876, Dec. 2005, doi: 10.1109/TAP.2005.859919.

[46] H. Barhom, C. Carmeli, and I. Carmeli, "Fabrication of Electronic Junctions between Oriented Multilayers of Photosystem i and the Electrodes of Optoelectronic Solid-State Devices," *J. Phys. Chem. B*, vol. 125, no. 3, pp. 722–728, Jan. 2021, doi: 10.1021/ACS.JPCB.0C08161/ASSET/IMAGES/LARGE/JP0C08161_0003.JPEG.

[47] A. Sarycheva, A. Polemi, Y. Liu, K. Dandekar, B. Anasori, and Y. Gogotsi, "2D titanium carbide (MXene) for wireless communication," *Sci. Adv.*, vol. 4, no. 9, Sep. 2018, doi: 10.1126/SCIADV.AAU0920/SUPPL_FILE/AAU0920_SM.PDF.

[48] G. P. Lim *et al.*, "Cytotoxicity of MXene-based nanomaterials for biomedical applications: A mini review," *Environ. Res.*, vol. 201, p. 111592, Oct. 2021, doi: 10.1016/J.ENVRES.2021.111592.

[49] C. E. Shuck, K. Ventura-Martinez, A. Goad, S. Uzun, M. Shekhirev, and Y. Gogotsi, "Safe Synthesis of MAX and MXene: Guidelines to Reduce Risk during Synthesis," *ACS Chem. Heal. Saf.*, vol. 28, no. 5, pp. 326–338, Sep. 2021, doi: 10.1021/ACS.CHAS.1C00051/SUPPL_FILE/HS1C00051_SI_002.PDF.

[50] G. A. Montgomery, M. W. Belitz, R. P. Guralnick, and M. W. Tingley, "Standards and Best Practices for Monitoring and Benchmarking Insects," *Front. Ecol. Evol.*, vol. 8, p. 579193, Jan. 2021, doi: 10.3389/FEVO.2020.579193/BIBTEX.

Dmitry Dobrykh was born in Perm, Russia, in 1995. He received the M.Sc. degree in radiophysics from ITMO University, St. Petersburg, Russia, in 2019. He is currently a PhD student with the School of Electrical Engineering, Tel Aviv University, Tel Aviv, Israel. His research interests include antennas and microwave devices, RFID, metamaterials, MRI, and topological photonics.

Hani Barhum is a Principal Investigator at the Triangle Research and Development Center. He he is a PhD student from Tel Aviv University, holds M.Sc. in Molecular Biology & Nanoscience, and a B.Sc. in Biophysics from the Hebrew University of Jerusalem, along with a B.Sc. in Chemistry. Dr. Specializes in the interdisciplinary fields of biophysics and material engineering, with a focus on the synthesis and design of optical materials.

Denis S. Kolchanov was born in Angarsk, Russia, in 1995. He received the M.Sc. degree in Chemical nanofabrication from ITMO University, SCAMT laboratory St. Petersburg, Russia, in 2019. He is currently a PhD student with the School of Electrical Engineering, Tel Aviv University, Tel Aviv, Israel. His current research interests include chemical fabrication, metallization, metamaterials, and photonics.

Or Messer holds a B.Sc. in mechanical engineering from Technion – Israel Institute of Technology and an M.Sc. in materials science and engineering from Ben-Gurion University. Currently pursuing a Ph.D. in materials science and engineering at Tel Aviv University. His focus is on MXene-based nanocomposites.

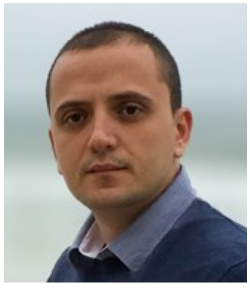

Maxim Sokol is a Senior Lecturer at Tel Aviv University's Department of Materials Engineering and Science, where he leads the Advanced Ceramics Laboratory. He received his Ph.D. in Materials Engineering from Ben-Gurion University in 2017. At the forefront of the Advanced Ceramics Laboratory, Dr. Sokol oversees a dynamic range of research activities. His laboratory is a hub for interdisciplinary research, delving into critical areas like nanomaterials and 2D materials, specifically focusing on MXenes. Other key research areas include ceramic matrix composites, advanced structural ceramics, and transparent ceramics.

Avigdor Drucker was born in Tel Aviv, Israel, in 1947. He received the B.Sc. degree in 1969, and the M.Sc. degree in 1977, both from the Technion, Israel Institute of Technology. He worked for many years as a microwave engineer, design, and management in the industry. He is currently the engineer and the manager of the RFIC laboratory in the School of Electrical Engineering, Tel Aviv University, Tel Aviv, Israel.

Eran Socher (Senior Member, IEEE) received the B.A. degree (summa cum laude) in physics and the B.Sc. (summa cum laude), M.Sc., and Ph.D. degrees in electrical engineering from the Technion-Israel Institute of Technology, Haifa, Israel, in 1996, 1996, 1999, and 2005, respectively, with a focus on CMOS compatible MEMS sensors and actuators and their readout electronics, especially for uncooled thermal imaging. From 2003 to 2006, he was a Research Engineer with Israel Defense Forces and an Adjunct Lecturer with Technion and Bar-Ilan University, Ramat Gan, Israel. From 2006 to 2008, he was a Visiting Researcher with High-Speed Electronics Laboratory and a Visiting Assistant Professor with the Department of Electrical Engineering, University of California at Los Angeles, Los Angeles, CA, USA. Since 2008, he has been with the School of Electrical Engineering, Tel Aviv University, Tel Aviv, Israel, where he is currently a Full Professor and Head of the School since 2023. He also heads the High Frequency Integrated Circuits and VLSI Laboratories.

Alexey Slobozhanyuk was born in St. Petersburg, Russia, in 1991. He received the B.Sc. degree in 2013 and M.Sc. degree in 2015 in photonics from ITMO University (Russia) and PhD in 2017 from Australian National University (Australia). He is currently an Assistant Professor at the ITMO University. His main research interests are applied electromagnetics, metamaterials, photonic topological insulators and metasurfaces.

Dmitry Filonov was born in Saint Petersburg, Russia, in 1991. He received the B.Sc. and M.Sc. degrees in photonics from ITMO University, Saint Petersburg, in 2013 and 2015, respectively, and the Ph.D. degree from Tel Aviv University, Tel Aviv, Israel, in 2019. He is currently the Head of the Radiophotonics Laboratory and an Assistant Professor with the Moscow Institute of Physics and Technology, Moscow, Russia. His main research interests include antenna, applied electromagnetics, all-dielectric structures, radio frequency identification (RFID), and metamaterials.

Pavel Ginzburg is an Associated Professor at Tel Aviv University. He is a former EPSRC Research Fellow, International Newton Research Fellow, and Rothschild Fellow at King's College London. He received his PhD from Technion in 2011. Pavel Ginzburg is the head of 'Dynamics of Nanostructures' Laboratory, encompassing theoretical group, optical spectroscopy, and radio waves labs. The Laboratory runs multidisciplinary research in the field of Bio photonics Quantum Mechanics, Nanoplasmonics and Metamaterials, Optical Forces and Radio Physics.